

HIL02K: TRANSPORT CROSS SECTIONS FOR NEUTRON ENERGIES TO 2 GEV

Richard A. Lillie
Oak Ridge Nat'l Lab
P. O. Box 2008
Oak Ridge, TN 37831 USA
(865) 574-6083
lilliera@ornl.gov

Franz X. Gallmeier
Oak Ridge Nat'l Lab
P. O. Box 2008
Oak Ridge, TN 37831 USA
(865) 574-9675
gallmeierfz@ornl.gov

Jeffrey O. Johnson
Oak Ridge Nat'l Lab
P. O. Box 2008
Oak Ridge, TN 37831 USA
(865) 574-5262
johnsonjo@ornl.gov

INTRODUCTION

For neutron energies above 20 MeV, measured doubly differential cross-section data is sparse and most accelerator neutronics calculations are performed using Monte Carlo codes employing high-energy stochastic collision models. Monte Carlo methods are very well suited for analyzing geometrically complex systems. However, often they are computationally expensive when used for accelerator shield design. This is particularly true in the preliminary stages of most designs when simple one-dimensional transport calculations are sufficient for conceptual studies. In these instances, deterministic discrete ordinates transport methods utilizing data in multigroup transport libraries are the preferred alternative to Monte Carlo.

For accelerator applications, multigroup transport libraries must contain both low- and high-energy transport cross sections and thus are built by combining both low energy measured data and high-energy calculated data. The low-energy cross sections are most often based on data contained in Evaluated Nuclear Data Files (ENDF) and the high-energy cross sections are most often generated from data calculated with high-energy stochastic collision models. HIL02k is a completely new high-energy neutron and photon transport library built in this manner for 32 nuclides. It contains 42 high- and 41 low-energy neutron groups and 22 photon groups for a total of 105 energy groups. A complete listing of the 32 nuclides and the energy group structure is given in Ref 1. HIL02k was developed as part of the neutronics R&D effort associated with the design of the Spallation Neutron Source (SNS)² currently under construction at ORNL.

In Section I, the methods employed to generate the doubly differential high-energy interaction and production data are briefly described. The methods employed to process the high-energy data are

discussed in Section II. In Section III, comparative results obtained during testing of HIL02k are presented and a brief summary is given in Section IV.

I. HIGH-ENERGY DATA GENERATION

The high-energy neutron interaction and doubly differential neutron and photon production data required to create HIL02k was generated using a modified version of MCNPX.³ All nonelastic collisions were treated using the Bertini intra-nuclear cascade, the multistage pre-equilibrium exciton, and the evaporation models in LAHET.⁴ All elastic collisions were treated using the nucleon nucleus elastic scattering model and all photon production was treated using the PHT photon production model in LAHET.

All of the MCNPX calculations were performed using a finite radius spherical model to allow particle transport. Particle transport was necessary to approximately account for the secondary neutrons produced by the charged particles exiting both primary (initial neutron interactions) and secondary collisions (charged particle interactions only). Normally, secondary neutrons produced by secondary charged particles are not treated when generating data for high-energy transport cross sections. However, as the incident neutron energy increases, the number of secondary neutrons produced a small distance from the initial interaction site also increases.

Most of the modifications to MCNPX were made to simply output data. However, a number of additional modifications were required for accounting purposes since particle transport was allowed. First, all primary collisions were forced to occur at the center of the 0.5 m radius sphere. This substantially increased efficiency by eliminating the large number of non-interacting incident particles

that arise when using a thin target approximation. Second, neutrons exiting either a primary or secondary collision were “killed” so that they could not be transported and possibly produce additional neutrons. Third, the kinetic energies of the charged particles both exiting and entering collisions were monitored to obtain data for kerma factors.

The high-energy neutron interaction and neutron and photon production data was generated using 43 discrete incident neutron energies above 19.64 MeV. Discrete incident neutron energies were employed to produce “point like” data. This allows the energy dependence of the incident neutrons to be easily varied after the doubly differential production data has been generated. The number of incident neutrons chosen at each incident energy for each nuclide was determined from an algorithm that attempted to predict the energy group (bin) boundaries such that each energy bin contained an equal number of secondary neutrons with equal uncertainties. This in turn allowed a fairly accurate estimate to be made of the number of incident neutrons required for acceptable uncertainties. (In this work, an uncertainty of 1% on each energy bin was assumed to be acceptable).

II. HIGH-ENERGY DATA PROCESSING

Most deterministic radiation transport codes employ Legendre polynomials to represent the angular dependence of the group-to-group scattering cross sections. Since the doubly differential particle production data produced by MCNPX was generated at discrete incident energies, the first step in processing this data was to obtain point-to-group Legendre coefficients to describe the angular dependence of produced neutrons (or photons). These coefficients were obtained directly from the individual particle data generated by MCNPX using a technique similar to that used by D. Filges, et. al.⁵ to construct discrete ordinates angular fluxes from Monte Carlo particle boundary crossing data. Each exiting neutron (or photon) was assumed to come from a single discrete scattering event. The contribution of each exiting neutron (or photon) to the n^{th} Legendre coefficient was thus obtained by simply evaluating the n^{th} Legendre polynomial at the cosine of the angle between the incident and exiting neutron (or photon) directions. The energy dependence or group structure of the Legendre coefficients was determined by tagging the contribution to each coefficient based on the energy bin containing the energy of the exiting particle. Once the point-to-

group particle production coefficients were determined, the point-to-group Legendre scattering coefficients were obtained by simply multiplying the nonelastic and elastic production coefficients by the appropriate nonelastic or elastic cross section.

Two versions of HILO2k were produced, i.e., standard and modified versions. In the standard version, all high-energy particle interaction and production data were taken into account (binned) to obtain the interaction cross sections and point-to-group coefficients. In the modified version, a neutron exiting a collision was ignored if the cosine of the angle between its direction and the incident neutron direction was greater than 0.99 and its kinetic energy was greater than 95% of the incident neutron energy. In addition, the collision producing this neutron was ignored in determining the corresponding interaction cross section. These rejection criteria were applied to all neutrons exiting both elastic and nonelastic interactions with all nuclides except H. Ignoring these neutrons results in reduced point-to-group scattering cross sections while ignoring the corresponding collisions results in reduced interaction cross sections. Reducing these cross sections in this manner is equivalent to assuming that these neutrons may be accurately represented as uncollided particles. The modified data sets were generated to help alleviate computational problems that sometimes occur in multi-dimension calculations when highly forward peaked scattering exists and low order Legendre polynomials are used to represent the angular dependence of scattering.

The second step in processing the high-energy particle production data consisted of converting the point-to-group scattering coefficients into group-to-group scattering coefficients. Since the incident neutron energies were chosen to be equal to the energy group boundaries, (requires no prior assumption regarding the collision distribution within a group) this step was first accomplished by simply averaging the point-to-group data generated at the upper and lower energies of each group. The scheme worked well in converting nonelastic point-to-group data to group-to-group data since the energy distributions of the neutrons exiting nonelastic collisions were fairly smooth and well behaved. However, for elastic collisions, the simple averaging scheme did not produce adequate scattering coefficients for within group scatter (self-scatter) or for scatter to the next lower energy group. Since the neutrons undergoing elastic

collisions lost very little energy, particularly in collisions with heavier nuclides, almost all of the incident neutrons colliding within a group remained in that group. In contrast, the simple averaging scheme placed half of these neutrons in the next lower group.

The problems associated with simple averaging were eliminated by employing equally sized subgroups in the group immediately below the incident neutron energy. Normally, if a neutron exiting an elastic collision self-scattered, it was treated as a single neutron and assigned a corresponding score of 1.0. However, with subgroups, its score was assigned based on which subgroup it entered. Thus, if the energy of the scattered neutron fell within the i^{th} subgroup, it was assigned a score given by the following relationship:

$$S_i = (N - i + 1/2) / N,$$

where N is the number of subgroups. This equation is based on three assumptions. First, the distribution of scattered neutrons in the subgroups immediately below the upper energy of any subgroup is the same as the distribution obtained in the corresponding subgroups immediately below the upper energy of the group. Second, the number of neutrons scattered within a subgroup that remain within the group is equal to the average of the number of neutrons scattered at the upper and lower energies of the subgroup that remain within the group. Third, the collision distribution within each group is constant.

Using a similar subgroup scheme to determine down-scatter to the next lower group is much more difficult unless the current group and next lower group are equal in size. Because of this, the elastic scatter to the next lower energy group was obtained by conserving the number of neutrons that scatter from the current group to all other groups. If it is assumed that the number of neutrons that down-scatter into all groups below the next lower group is correct using simple averaging, then the change in the number of neutrons that down-scatter to the next group must be equal to the negative change in the number that self-scatter. Thus, once the number of neutrons that self-scatter was determined using subgroups, the difference between this value and the value obtained using simple averaging was subtracted from the “simple

averaging” number that down-scatter to the next group.

The effects of using subgroups to improve the elastic scattering coefficients for within group self-scatter and down-scatter to the next group were determined by performing transport calculations employing three different modified versions of the HILO2k library. The three versions contained high-energy elastic group-to-group cross sections generated using 1) simple averaging of the point-to-group data, 2) subgroups for only the elastic self-scatter, and 3) subgroups for the elastic self-scatter and corrected down-scatter to the next group. The model employed in these calculations consisted of a point isotropic neutron source uniformly distributed in energy between 60 and 70 MeV and located at the center of a spherical 17 m thick regular concrete shield. Dose rates obtained using the deterministic one-dimensional discrete ordinates code ANISN⁶ with HILO2k are compared with those obtained using MCNPX in Fig. 1.

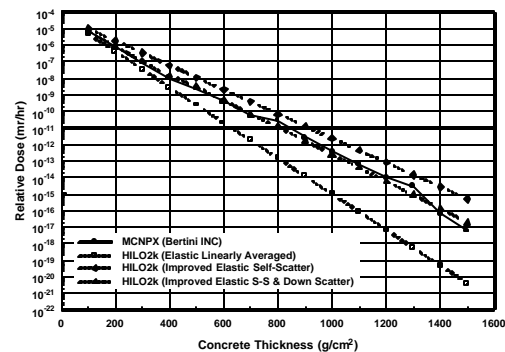


Figure 1. Relative Dose Rates in Concrete Shield

Dose rates are only presented out to a distance of 6.4 m (1500 g/cm²) since adequate statistics could not be obtained with MCNPX beyond this distance for reasonable run times. Without the use of subgroups, ANISN underestimates the dose rate at 1500 g/cm² by more than a factor of 1000. With the cross-section set containing improved elastic self-scatter, ANISN overestimates the dose rate by about a factor of 100 at 1500 g/cm². For the cross-section set containing both improved elastic self-scatter and down-scatter to the next group, excellent agreement is obtained between the ANISN and MCNPX calculated dose rates.

III. HILO2K TESTING

A number of calculations have been carried out to test HILO2k. In the most severe tests, the dose rate throughout a one-dimensional spherical model of the SNS target monolith was calculated with ANISN using both versions of HILO2k and compared with the dose rate calculated with MCNPX. The actual model employed in the calculations simulated an early design of the target monolith. This design consisted of the Hg target, the water-cooled Pb reflector, the water-cooled inner steel shield, the steel bulk shield, and the outer concrete shield. A point isotropic neutron source uniformly distributed in energy between 950 and 1000 MeV was placed in the center of the Hg to simulate 1 GeV protons incident on the SNS Hg target. Space- and energy-dependent weight windows based on adjoint fluxes calculated with ANISN were employed in the MCNPX calculations. Calculations were also performed after replacing the 1020 steel in the outer shield with SS 304. The results from these calculations are presented in Figs. 2 and 3.

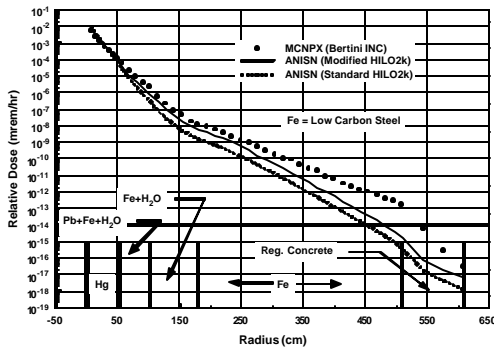


Figure 2. Dose Rates in 1-D Spherical Model of SNS Target Monolith.

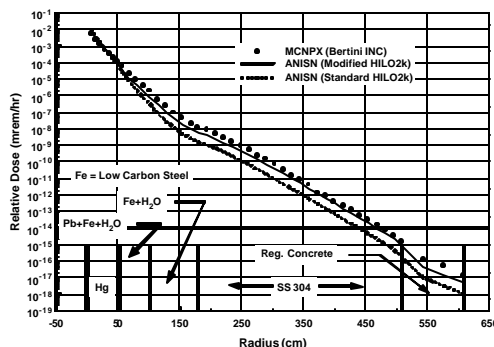


Figure 3. Dose Rates in 1-D Spherical Model of Modified SNS Target Monolith.

In Fig. 2, the dose rate calculated using the modified version of HILO2k agrees fairly well with the dose rate calculated with MCNPX out to the beginning of the 1020 steel (shown as Fe in Fig. 2). From this point outward, the dose rate calculated with HILO2k falls off much more rapidly than that calculated with MCNPX and at the outer edge of the 1020 steel, HILO2k underestimates the dose rate by approximately two orders of magnitude. The reason for this drastic difference is that the dose rate at the outer edge of the Fe is dominated by low-energy neutrons “filtering” through the Fe unresolved resonance region. The low energy group structure in HILO2k is too coarse to allow adequate representation of this region whereas the point cross-section data in MCNPX does represent this region adequately. This explanation is borne out in the concrete where the MCNPX calculated dose rate is attenuated much more rapidly than that calculated with HILO2k. This explanation is further evidenced by the results obtained with the SS 304. Since SS 304 only contains about 65 percent Fe, versus 99 percent in 1020 steel, much better agreement is obtained between the ANISN and MCNPX calculated dose rates. As expected, in both sets of calculations, the standard library predicts lower dose rates than the modified library.

IV. SUMMARY

HILO2k is a new transport cross-section library that contains ANISN formatted cross sections for neutron energies up to 2 GeV. The cross sections for neutron energies above 20 MeV are based on neutron interaction data obtained from MCNPX. Below 20 MeV, these cross sections are based on evaluated data. Testing of the library illustrates the important role that multigroup transport cross sections can play in high-energy preliminary shielding design applications as use of the stochastic models in MCNPX required over 220 thousand times as much cpu time as ANISN.

REFERENCES

1. R. A. Lillie and F. X. Gallmeier, “HILO2k: A Coupled Neutron-Photon Transport Cross-Section Library for Neutron Energies up to 2000 MeV,” *Proc. 4th Int. Top. Meet. Nucl. Applicat. of Accel. Tech.*, p 302-309, Nov. 12-15, 2000, Washington, DC (2000).

2. B. R. Appleton, "National Spallation Neutron Source Conceptual Design Report Vol. 1," ORNL Report ORNL/TM-6063, Oak Ridge, TN (1997).
3. F. X. Gallmeier, "Implementation of the CEM-Code into the MCNPX-Code," *Proc. 4th Work. on Simul. Accel. Rad. Envir.*, p. 131-129, Sept. 14-16, 1998, Knoxville, TN (1998).
4. R. E. Prael and H. Lichtenstein, "Users Guide to LCS: The LAHET Code System, LANL Report LA-UR-89-3014, Los Alamos, NM (1989).
5. D. Filges, R. D. Neef, H. Schaal, and B. Wolfertz, "Procedures and Data for Shielding Calculations of Spallation Target Stations and Accelerators in the Medium Energy Range," *Proc. Spec. Meet. Shield. Aspects of Accel., Targ. & Irrad. Facil.*, p. 253-270, Apr. 28-29, 1994, Arlington, TX (1994).
6. W. W. Engle, Jr., "ANISN, A One-Dimensional Discrete Ordinates Transport Code with Anisotropic Scattering," ORGDP Report K-1693, Oak Ridge, TN (1967).